Restricted Rotation in Unbridged Sandwich Complexes: Rotational Behavior of *closo*-[Co(η^5-NC_4H_4)($C_2B_9H_{11}$)] Derivatives

Clara Viñas,[a] Jordi Llop,[a] Francesc Teixidor,*[a] Raikko Kivekäs,[b] and Reijo Sillanpää[c]

Abstract: Rotation about the centroid/metal/centroid axis in ferrocene is facile; the activation energy is 1–5 kcal mol^{-1}. The structurally similar sandwich complexes derived from *closo*-[3-Co(η^5-NC_4H_4)-1,2-$C_2B_9H_{11}$] (**1**) have a different rotational habit. In **1,** the *cis* rotamer in which the pyrrolyl nitrogen atom bisects the carboranyl cluster atoms is 3.5 kcal mol^{-1} more stable in energy than the rotamer that is second lowest in energy. This *cis* rotamer is wide, spanning 216°, and may be split into three rotamers of almost equal energy by substituting the N and the carboranyl carbon atoms adequately. To support this statement, *closo*-[3-Co(η^5-NC_4H_4)-1,2-$(CH_3)_2$-1,2-$C_2B_9H_9$] (**2**), *closo*-[3-Co(η^5-NC_4H_4)-1,2-$(\mu$-$CH_2)_3$-1,2-$C_2B_9H_9$] (**3**), **2**→BF_3, and **3**→BF_3 have been prepared. Two rotamers are found at low temperature for **2**→BF_3 and **3**→BF_3. Compounds **2**, **3**, and **1**→BF_3 behave similarly to **1**. Rotational energy barriers and the relative populations of the different energy states are calculated from ^{1}H DNMR spectroscopy (DNMR, dynamic NMR). These results agree with those of semiempirical calculations. Without exception, the *cis* rotamer is energetically the more stable. The fixed conformation of **1** assists in elucidating the rotational preferences of the [3,3′-Co(1,2-$C_2B_9H_{11})_2$]$^-$ ion in the absence of steric hindrance; the [3,3′-Co(1,2-$C_2B_9H_{11})_2$]$^-$ ion is commonly accepted to present a *cisoid* orientation. Complex **1** is electronically similar to the [3,3′-Co(1,2-$C_2B_9H_{11})_2$]$^-$ ion. Both have heteroatoms in the π ligands, and they have the same electronegativity difference between the constituent atoms. This leads to a view of the [NC_4H_4]$^-$ as [7,8-$C_2B_9H_{11}$]$^{2-}$ ion, with no steric implications. Therefore the [3,3′-Co(1,2-$C_2B_9H_{11})_2$]$^-$ ion should be considered to have a *cisoid* structure, and the different rotamers observed to be the result of steric factors and of the interaction of the counterion with either B–H groups and/or ancillary ligands. The rotamer adopted is the one with the atoms holding the negative charges furthest apart.

Keywords: carboranes · conformation analysis · rotation barrier · sandwich complexes · structure elucidation

Introduction

The scientific literature on the η^5-cyclopentadienyl ligand (Cp) is extraordinarily large; of all its complexes ferrocene is the best known,[1] having a rich derivative chemistry.[2] One of the characteristics of ferrocene and its derivatives is the easy rotation[3] of one ring relative to the other, with energy barriers of 1–5 kcal mol^{-1}[4] comparable to those of ethane.[5] To slow down or restrict this facile rotation it is necessary to generate overcrowding or ring–ring bridging spacers in the molecule.[6]

Besides Cp and its analogue Cp*, not many η^5 anionic ligands are available. η^5-[$C_2B_9H_{11}$]$^{2-}$,[7] η^5-[NC_4H_4]$^-$ ions,[8] and their derivatives are considerably less used.[9] Similarly to the case of ferrocene, a great number of sandwich complexes [3,3′-M(1,2-$C_2B_9H_{11})_2$]$^{z-}$ (M = transition metal) exist. Of the three sandwich complexes in Figure 1, [3,3′-Co(1,2-$C_2B_9H_{11})_2$]$^-$ has been the most thoroughly studied; the number of derivatives and structural data available is surprising.[9d] Three possible orientations of the carborane cages in the complexes are possible: *transoid*, *cisoid*, and *gauche*. The limiting *cisoid* and *transoid* orientations are the most commonly encountered, but it is not clear which one is

[a] Dr. C. Viñas, Dr. J. Llop, Prof. F. Teixidor
Institut de Ciència de Materials de Barcelona
Consejo Superior de Investigaciones Científicas
Campus de U.A.B., Bellaterra, 08193 Barcelona (Spain)
Fax: (+34) 93-580-5729
E-mail: teixidor@icmab.es

[b] Dr. R. Kivekäs
Inorganic Chemistry Laboratory, Box 55, University of Helsinki
00014 Helsinki (Finland)

[c] Prof. R. Sillanpää
Department of Chemistry, University of Jyväskylä
40351 Jyväskylä (Finland)

 DOI: 10.1002/chem.200400445

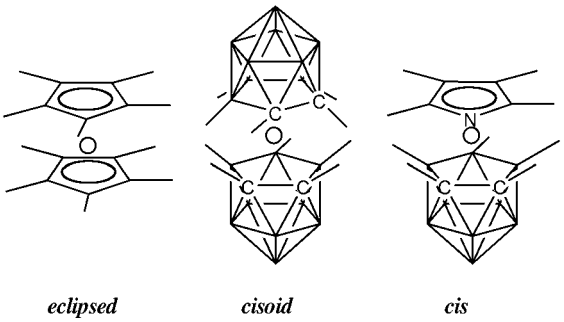

Figure 1. Schematic representation of $[FeCp_2]$, $[3,3'\text{-}Co(1,2\text{-}C_2B_9H_{11})_2]^-$, and $[3\text{-}Co(\eta^5\text{-}NC_4H_4)\text{-}1,2\text{-}C_2B_9H_{11}]$ (**1**). The circle represents the metal ion, Fe in ferrocene and Co for the other two. Lines radiating from the pentagonal coordinating faces are indicative of the steric repulsion expected.

the most preferred: different authors give contradictory interpretations.[9d,10]Steric factors are doubtless very relevant but the electronic contribution is not negligible, as exemplified by the crystal structure of $[Et_3NH]$ $[3,3'\text{-}Co(1,2\text{-}C_2B_9H_{11})_2]$,[11] Co^{III}, d^6, that is *cisoid*, as compared with $[Cs(dme)_4]_2[3,3'\text{-}Co(1,2\text{-}C_2B_9H_{11})_2]$,[10b] Co^{II}, d^7, that is *transoid*, or the molecular structures of $[3,3'\text{-}Ni(1,2\text{-}C_2B_9H_{11})_2]^-$, Ni^{III} d^7, *transoid*, or $[3,3'\text{-}Ni(1,2\text{-}C_2B_9H_{11})_2]$, Ni^{IV} d^6, *cisoid*.[10c]

The first mixed-sandwich compound incorporating an η^5-pyrrolyl unit and a dicarbollide unit, *closo*-$[3\text{-}Co(\eta^5\text{-}NC_4H_4)\text{-}1,2\text{-}C_2B_9H_{11}]$ (**1**; see Figure 1), was synthesized and characterized in 1996.[12] Since then, several derivatives of **1** have been synthesized; the resulting mixed-sandwich compounds are very stable.[13] For most of the derivatives of **1**, it has been found that the N bisects the $C_c\cdots C_c$ connection in the dicarbollide. It has a *cis* disposition of the heteroatoms. This constancy in the motif is rare in sandwich complexes with no ligand–ligand bridge.[9d] Therefore the pyrrolyl/dicarbollide combination could introduce novel geometric features to the sandwich complexes. This, along with the easy preparation of **1**, could open up new possibilities not encountered in the sandwich compounds commonly available.

Here, we report experiments on the capacity of **1** or its derivatives to rotate. The existence of two heteroatoms (C) on the dicarbollide unit and one heteroatom (N) on the pyrrolyl moiety led to the hypothesis that ring rotation would be more restricted than in ferrocene. Further, we show through the orientation of the ligands in **1** that if electronic factors alone are considered, the orientation of the ligands in $[3,3'\text{-}Co(1,2\text{-}C_2B_9H_{11})_2]^-$ would be *cisoid*. To prove it, experiments were designed to lower the rotation rate, to alter the activation energy, and to equalize the energy of the different rotamers. These experiments require NMR studies at variable temperature, and the synthesis of new mixed-sandwich complexes with steric hindrances at special sites. In this context, *closo*-$[3\text{-}Co(\eta^5\text{-}NC_4H_4)\text{-}1,2\text{-}(CH_3)_2\text{-}1,2\text{-}C_2B_9H_9]$ (**2**) and *closo*-$[3\text{-}Co(\eta^5\text{-}NC_4H_4)\text{-}1,2\text{-}(\mu\text{-}CH_2)_3\text{-}1,2\text{-}C_2B_9H_9]$ (**3**), as well as their $N\rightarrow BF_3$ adducts **2**$\rightarrow BF_3$ and **3**$\rightarrow BF_3$, were synthesized and studied by ^1H DNMR spectroscopy. The experimental work was complemented and tested with theoretical studies providing the energy of the possible conformers.

Results and Discussion

The first indication that **1** could have a more restricted rotational capacity than ferrocene was provided by its molecular structure obtained by X-ray diffraction, which revealed that the nitrogen atom was bisecting the two cluster carbon atoms (C_c). The three heteroatoms, that is, the N in the pyrrolyl and the two C_c atoms in the dicarbollide, were in a *cis* disposition. Likewise, in the molecular structures[13] of the similar, but nonsymmetrical, complexes *closo*-$[3\text{-}Co(\eta^5\text{-}NC_4H_4)\text{-}1\text{-}CH_3\text{-}2\text{-}C_4H_9\text{-}1,2\text{-}C_2B_9H_9]$ and *closo*-$[3\text{-}Co(\eta^5\text{-}NC_4H_4)\text{-}1\text{-}C_6H_5\text{-}2\text{-}C_3H_5\text{-}1,2\text{-}C_2B_9H_9]$, the nitrogen atom was in a *cis* disposition, too. The prevalence of the same structural motif in the three structures suggested that the *cis* rotamer was the most stable of all possible rotamers, and for **1** it was the most symmetrical rotamer accessible.

In solution, the NMR studies support the same conclusions. The room-temperature ^1H NMR spectrum of **1** is compatible with symmetrical rotamers only, as only two single resonances in the pyrrolyl region with an area ratio 2:2 are observed. The $^{13}C\{^1H\}$ NMR spectrum also presents two signals for the same moiety. These results are in agreement with a symmetric rotamer, but a relatively fast rotation of the pyrrolyl ring compared with the dicarbollide unit could not be ruled out. The ^1H DNMR study of **1** in the range 293–193 K did not provide any signal unfolding; the only observed effect was the linear shift with T^{-1} of NMR resonances. An energy profile of **1** as a function of the rotation angle α (Figure 2) was produced by semiempirical calculations to complement the experimental NMR data. The angle α is set to zero when N bisects the $C_c\cdots C_c$ connection. These calculations have shown that two gross rotamers, $\mathbf{A_2}$ and **B**, exist (Figure 3). In rotamer $\mathbf{A_2}$, as a sum of $\mathbf{a_i}$ conformations, the nitrogen atom oscillates between the boron atoms neigh-

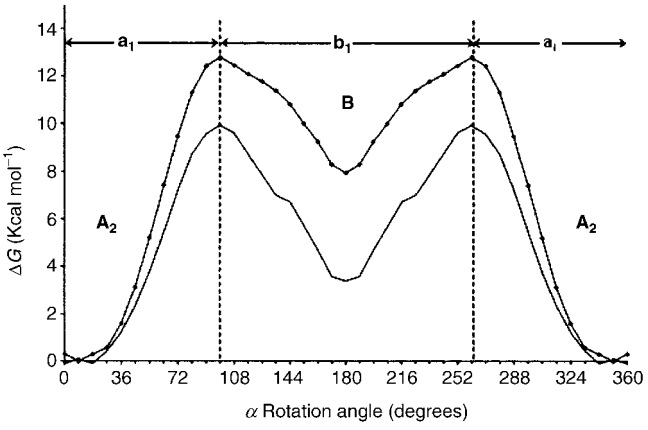

Figure 2. Energy profiles for *closo*-$[3\text{-}Co(\eta^5\text{-}NC_4H_4)\text{-}1,2\text{-}C_2B_9H_{11}]$ (**1**) (continuous line) and **1**$\rightarrow BF_3$ (dotted line) calculated by the ZINDO/1 method.

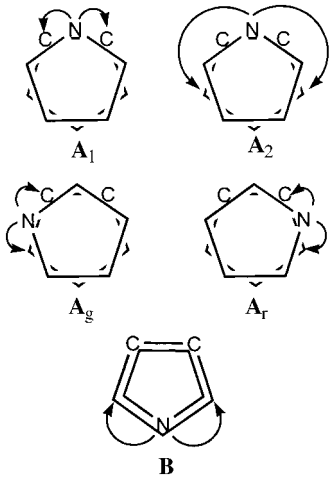

Figure 3. Possible rotamers in which mixed cobalt complexes and their derivatives are found. For simplicity only the five-member faces are shown. The pentagons with the two carbon atoms represent the [7,8-$C_2B_9H_{11}]^{2-}$ moiety. The arrows show the amplitude of the relative motion of the pyrrolyl moiety in each rotamer.

boring the carbon atoms of the cluster, staying close to the $C_c\cdots C_c$ edge, where $108° \leq \alpha \leq -108°$; in rotamer **B**, as a sum of $\mathbf{b_i}$ conformations, $108° \leq \alpha \leq 252°$. Rotamer $\mathbf{A_2}$ is 3.5 kcal mol^{-1} more stable than **B**, with a rotational barrier of 10 kcal mol^{-1}. This implies that rotamer **B**, in the temperature range 293–193 K, is not sufficiently populated[14] to be observed in NMR spectroscopy, and only molecules in rotamer $\mathbf{A_2}$ are found. This represents a major difference from ferrocene, even though the small rotational barrier does not prevent the pyrrolyl moiety from turning 360° with respect to the carboranyl moiety. Then, contrarily to ferrocene, there is a predominant rotamer $\mathbf{A_2}$ in **1** that we have described as a gross rotamer, considering that it spans nearly 216°, although its more stable conformation is like those found by X-ray diffraction. To confirm that the theoretical predictions matched the experimentation, investigations aimed to reduce the span of the rotation from 216° to 72° were undertaken. This situation is represented by $\mathbf{A_1}$ or $\mathbf{A_g}$/$\mathbf{A_r}$ in Figure 3. The span of rotation in $\mathbf{A_1}$ is $36° \leq \alpha \leq -36°$ and it is symmetric, in $\mathbf{A_g}$ it is $108° \leq \alpha \leq 36°$, and in $\mathbf{A_r}$ it is $-36° \leq \alpha \leq -108°$. $\mathbf{A_g}$ or $\mathbf{A_r}$ individually is not symmetric but $\mathbf{A_g}$ plus $\mathbf{A_r}$ present an apparently symmetric conformation. They generate a racemic global rotamer. The generation of $\mathbf{A_g}$/$\mathbf{A_r}$ is possible if the *cis* rotamer $\mathbf{A_2}$ is no longer the most stable.

Destabilization of the *cis* rotamer:

a) *Monosubstitution*: In **MS** (Figure 4), substitution on the pyrrolyl N atom with BF_3 leaves the charge on the complex unaltered. The fast reaction of **1** with $(C_2H_5)_2O\rightarrow BF_3$ affords **1**→BF_3. Its room-temperature ^{1}H NMR spectrum produced two signals in the pyrrolyl region with an area ratio of 2:2. Similarly to **1**, no signal unfolding was observed in the temperature range 293–193 K. Consequently, the synthesis of **1**→BF_3 did not produce remarkable changes from **1** in solution. The calculated energy profiles for **1** and **1**→BF_3 are very similar. In **1**→BF_3 the energy difference between $\mathbf{A_2}$ and **B** (8 kcal mol^{-1}) and the rotation energy barrier (13 kcal mol^{-1}) are augmented with respect to **1**.

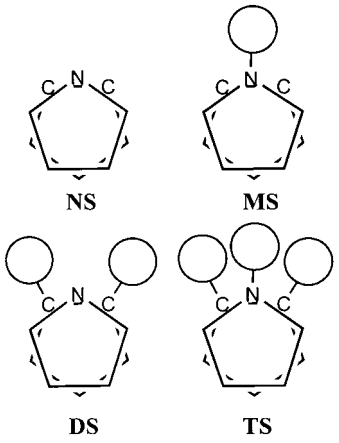

Figure 4. Schematic representation of the substitutions performed.

b) *Disubstitution*: In **DS** (Figure 4), substituents are introduced on the C_c atoms. With this aim, mixed sandwich compounds *closo*-[3-Co(η^5-NC_4H_4)-1,2-$(CH_3)_2$-1,2-$C_2B_9H_9$] (**2**) and *closo*-[3-Co(η^5-NC_4H_4)-1,2-(μ-$CH_2)_3$-1,2-$C_2B_9H_9$] (**3**) were synthesized by the established procedure.[12] Scheme 1 a

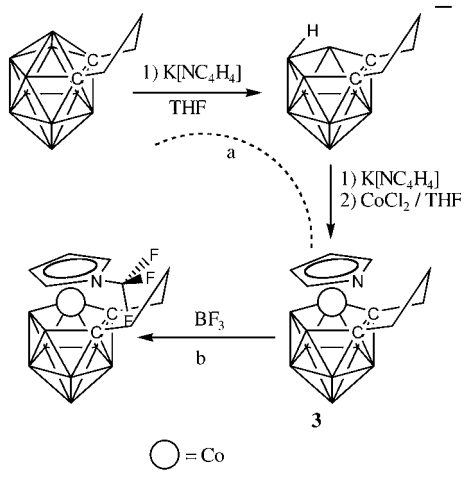

Scheme 1. a) Synthesis of compound **3**; b) reaction proposed for the formation of the adduct between **3** and BF_3.

shows the synthesis of **3**. The room-temperature ^{11}B NMR spectrum of **3** displays a 1:1:2:2:3 pattern, in agreement with C_s symmetry, in the δ range +8 to −17, consistently with derivatives of **1**. The ^{11}B NMR spectrum of **2** displays a similar 1:1:2:2:3 pattern. The room-temperature ^{1}H NMR spectra of **2** and **3** display two signals in the pyrrolyl region with an area ratio of 2:2 and, as was the case with **1**, no ^{1}H NMR signal unfolding was obtained in ^{1}H DNMR studies. Therefore, the incorporation of substituents on both cluster

carbon atoms introduces no substantial modifications in the habit of these complexes in solution. The X-ray structures of **2** and **3** confirmed that in the motif observed, the nitrogen bisects the $C_c\cdots C_c$ connection. The molecular structures of **2** and **3** (Figures 9 and 10) are described briefly at the end of this section.

c) *Trisubstitution*: In **TS** (Figure 4), substitution on the C_c atoms and on the N atom leave the charge on the complex unaltered. In this case, the triangular face C_cNC_c would be overcrowded, and high destabilization of conformer $\mathbf{A_2}$ could be expected. The **2**→BF_3 and **3**→BF_3 adduct complexes were prepared similarly to **1**→BF_3. The synthesis of **3**→BF_3 is shown in Scheme 1(b).

The ^{1}H NMR spectrum of **2**→BF_3 above 265 K (Figure 5) displays three singlets with area ratio 2:2:6, compatible with

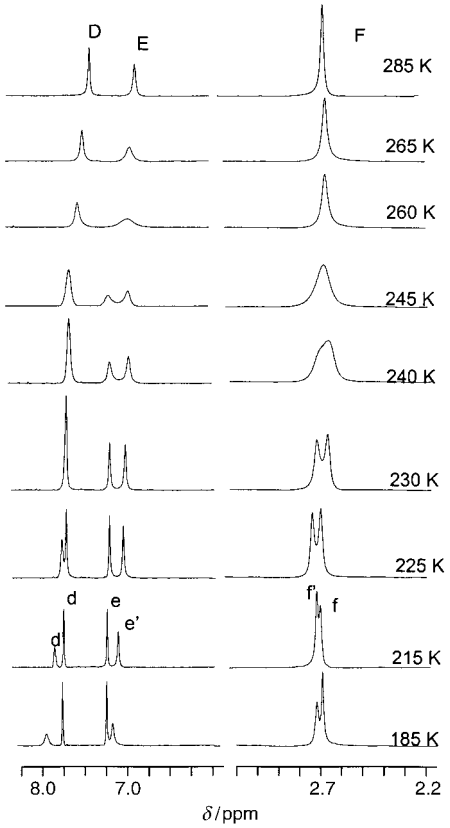

Figure 5. ^{1}H NMR spectra of **2**→BF_3 as a function of temperature. The resonances (d, e, f) and (d′, e′, f′) belong to the $\mathbf{A_g}/\mathbf{A_r}$ and $\mathbf{A_1}$ rotamers in Figure 4.

C_s symmetry. The two downfield resonances correspond to the pyrrolyl ring proton atoms and the third corresponds to the methyl groups on C_c. The ^{1}H DNMR study in the range 285–185 K proved to be very informative in this case. The spectrum at 225 K consists of six signals with area ratios **1.4**:2:2:**1.4**:**4.2**:6. Bold numbers correspond to one set of signals, plain numbers to the second set. The intensities change to **2.7**:2:2:**2.7**:6:**8.1** at 185 K. Therefore, the two participating sets of signals are dependent on the temperature, indicating that two energetically close rotamers co-exist but do not have precisely the same energy and degeneracy; otherwise they would always have the same populations. The resonance D (see Figure 5) de-coalesces at 227 K. The signal intensity distribution below 227 K indicates the co-existence of two rotamers: $\mathbf{A_g}/\mathbf{A_r}$[15] and $\mathbf{A_1}$ (see Figure 3). Rotamer $\mathbf{A_1}$ is symmetric, but $\mathbf{A_g}$ and $\mathbf{A_r}$ are not; however, fast interchange between $\mathbf{A_g}$ and $\mathbf{A_r}$ also produces a symmetry-averaged rotamer. Resonances d′, e′, and f′ correspond to the $\mathbf{A_g}/\mathbf{A_r}$ rotamers, as evidenced by the widening of these resonances at 185 K, below which each should split in two to account for the asymmetry of the $\mathbf{A_g}$ or $\mathbf{A_r}$ rotamer. If the two rotamers $\mathbf{A_g}/\mathbf{A_r}$ and $\mathbf{A_1}$ are close in energy and exist in almost equally probable states, as is the case here, K_c can be calculated at the coalescence temperature.[16] The frequency shifts of the signals are shown in Figure 6. Accordingly, $\Delta G^{\neq}$

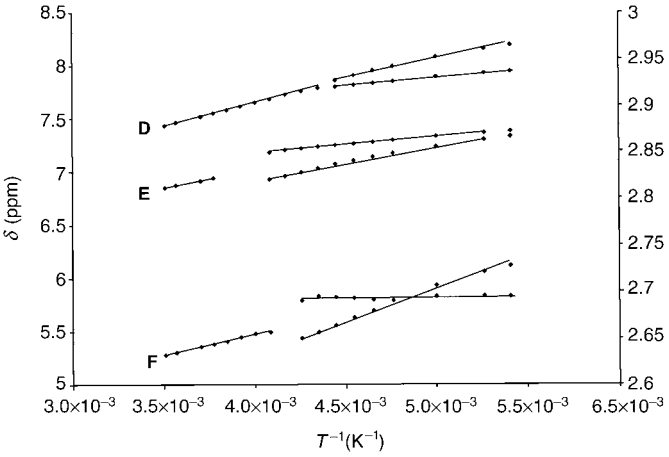

Figure 6. Proton shift before and after coalescence for **2**→BF_3. Chemical shifts on the left-hand scale are for resonances E and **D**. The right-hand scale is for resonance F.

for rotamer exchange can be calculated at the coalescence temperature from the three distinct sets of coalescence data D, E, and F (Table 1).[8b] From resonances E and F an average value, $\Delta G^{\neq} = 12.4 \pm 0.2$ kcal mol^{-1}, has been calculated. With the synthesis of the sterically crowded **2**→BF_3 it has been possible to differentiate between the two rotamers $\mathbf{A_1}$ and $\mathbf{A_g}/\mathbf{A_r}$ with similar energies down to 227 K, and the later splitting of one of them into two others at temperatures below 185 K can be envisaged.

Table 1. Calculation of rotational barrier for **2**→BF_3 and **3**→BF_3.

Compound	Signal	Coalescence temp. [K]	Δν [Hz][a]	$\Delta G^{\neq}$ [kcal mol^{-1}]
2→BF_3	E	255.0±2	92±1	12.4±0.2
	F	240.0±2	16±1	12.4±0.2
3→BF_3	D	257.5±2	51±1	13.0±0.2
	E	265.0±2	117±1	13.0±0.2

[a] Extrapolated to coalescence temperature.

To assist in the interpretation of these data, calculations leading to the energy profile for **2**→BF_3 (Figure 7) have produced remarkably similar results to those for **3**→BF_3. Five minima at 0°, 63°, 148°, 212°, and 297° are observed,

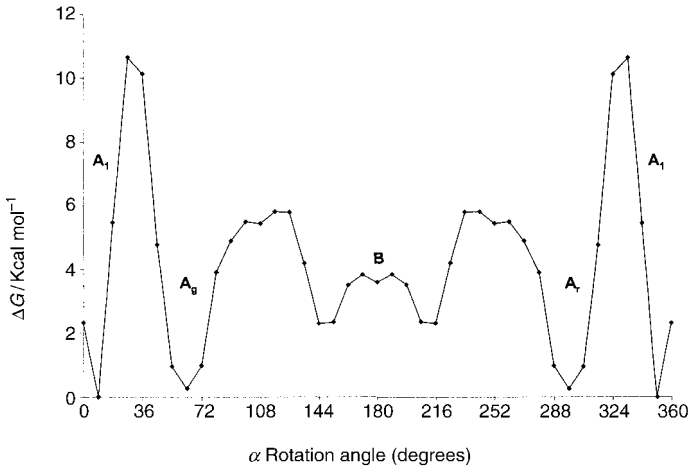

Figure 7. Calculated energy profile for **3**→BF_3 obtained by the ZINDO/1 method.

but the global minimum is found at 0°, corresponding to rotamer $\mathbf{A_1}$, very close in energy (<0.3 kcal mol^{-1}) to those at 63° and 297° corresponding to enantiomeric rotamers $\mathbf{A_g}$ and $\mathbf{A_r}$. The minima at 0° and 63° are separated in **2**→BF_3 by a barrier of 9 kcal mol^{-1}. $\mathbf{A_g}$ and $\mathbf{A_r}$ are separated by 5 kcal mol^{-1} activation energy, which facilitates their rapid exchange below 185 K. Therefore the ^{1}H DNMR spectra of **2**→BF_3 (Figure 5) is in full agreement with this energy profile. Rotamers $\mathbf{A_1}$ and $\mathbf{A_g}/\mathbf{A_r}$ exchange rapidly at $T>255$ K, producing an averaged $\mathbf{A_2}$ rotamer. This exchange is frozen at $T<240$ K when rotamers $\mathbf{A_1}$, and $\mathbf{A_g}/\mathbf{A_r}$ co-exist but do not exchange with each other. At 185 K the enantiomeric rotamers $\mathbf{A_g}$ and $\mathbf{A_r}$ still exchange rapidly; to freeze this exchange it is necessary to lower the temperature. This explanation permits assignment of the sets of resonances (d, e, f) to $\mathbf{A_1}$ and (d′, e′, f′) to the racemic $\mathbf{A_g}/\mathbf{A_r}$.

Similar results were obtained with **3**→BF_3, although the ^{1}H DNMR spectrum of **3**→BF_3 is more complicated owing to the spin–spin coupling between methylene groups. To simplify the study only those signals corresponding to the pyrrolyl hydrogen atoms have been taken into account (Figure 8). The variable-temperature spectra can be interpreted as for **2**→BF_3. Two singlets were observed above 265 K, and four singlets below 250 K, with area ratios of 2:**5.9**:2:**5.9** at 250 K and **1.7**:2:2:**1.7** at 185 K. The existence of two rotamers, $\mathbf{A_1}$ and $\mathbf{A_g}/\mathbf{A_r}$, also explains the resonances and area ratios obtained. The values of T_c, K_c, and $\Delta G^{\neq}$ are summarized in Table 1. Both **2**→BF_3 and **3**→BF_3 have similar $\Delta G^{\neq}$ values near 13.0 kcal mol^{-1}. For **2**→BF_3 the two sets of resonances (d, e) and (d′, e′) were assigned to $\mathbf{A_g}/\mathbf{A_r}$ and $\mathbf{A_1}$ respectively.

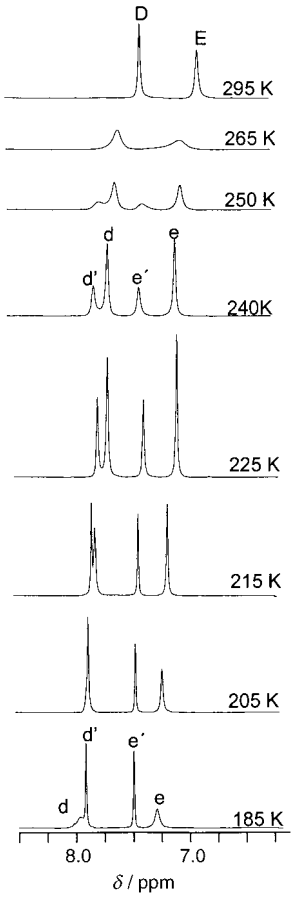

Figure 8. ^{1}H NMR spectra of **3**→BF_3 as a function of temperature. The resonances (d, e) and (d′, e′) belong to the $\mathbf{A_g}/\mathbf{A_r}$ and $\mathbf{A_1}$ rotamers in Figure 4.

The crystal structures: The expected structures, with the pyrrolyl nitrogen placed approximately between the cluster carbons, were confirmed. Selected bond lengths and angles are listed in Table 2, crystallographic data are in Table 3, and **2** and **3** are represented in Figures 9 and 10, respectively. For both compounds, the pyrrolyl ligand and the coordinated C_2B_3 face are not parallel but tilted so that the pyrrolyl nitrogen has moved away from the cluster carbons. This is one of the sources of error in the computational analysis, as both faces have been assumed parallel to simplify the calcula-

Table 2. Selected bond lengths [Å] and angles [°] for **2** and **3**.

	2	**3**
Co3–N13	2.070(3)	2.093(4)
Co3–C1	2.025(3)	2.044(4)
Co3–C2	2.024(3)	2.048(4)
Co3–C15	2.050(3)	2.061(5)
Co3–C16	2.050(3)	2.043(5)
Co3–B8	2.073(4)	2.062(5)
C1–C2	1.669(4)	1.635(6)
C1-Co3-N13	108.45(13)	111.46(18)
C2-Co3-N13	108.65(13)	108.15(18)
C15-Co3-B8	97.26(16)	98.4(2)
C16-Co3-B8	97.16(16)	94.8(2)

Table 3. Crystallographic data for **2** and **3**.

Complex	**2**	**3**
empirical formula	$C_8H_{19}B_9CoN$	$C_9H_{19}B_9CoN$
formula weight	285.46	287.47
crystal system	monoclinic	orthorhombic
crystal habit, color	prism, red	needle, red
space group	$P2_1/n$ (no. 14)	$P2_12_12_1$ (no. 19)
a [Å]	8.5064(8)	11.7484(13)
b [Å]	14.2273(14)	15.947(2)
c [Å]	12.0139(5)	7.8015(17)
β [°]	92.352(5)	90
V [Å^3]	1452.7(2)	1461.6(4)
Z	4	4
T [°C]	21	21
λ [Å]	0.71069	0.71069
ρ [g cm^{-3}]	1.305	1.352
μ [cm^{-1}]	11.54	11.51
goodness-of-fit[a] on F^2	1.020	1.052
R[b] $[I>2\sigma(I)]$	0.0357	0.0326
R_w[c] $[I>2\sigma(I)]$	0.0785	0.0812

[a] $S = [\Sigma(w(F_o^2-F_c^2)^2]/(n-p)^{1/2}$. [b] $R = \Sigma||F_o|-|F_c||/\Sigma|F_o|$. [c] $R_w = [\Sigma w(|F_o^2|-|F_c^2|)^2/\Sigma w|F_o^2|^2]^{1/2}$.

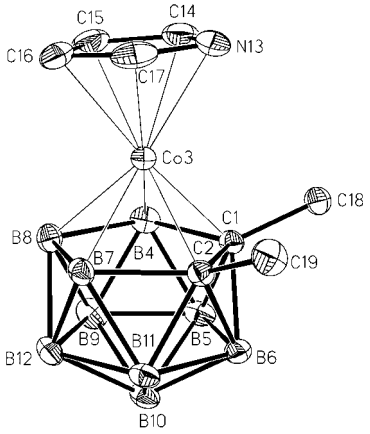

Figure 9. Molecular structure of *closo*-[3-Co(η^5-NC_4H_4)-1,2-$(CH_3)_2$-1,2-$C_2B_9H_9$] (**2**).

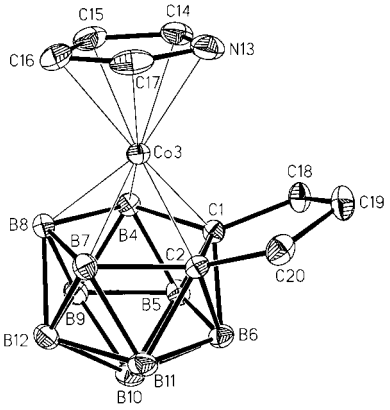

Figure 10. Molecular structure of *closo*-[3-Co(η^5-NC_4H_4)-1,2-(μ-CH_2)$_3$-1,2-$C_2B_9H_9$] (**3**).

tions. As a result of this tilting, the dihedral angle between the two coordinated pentagonal faces is 6.4(2)° for **2** and 8.3(3)° for **3**. These are set to 0°, θ = 180°, to run the energy profile calculations. For **2**, the pyrrolyl nitrogen is placed exactly midway between the cluster carbons, and the bond parameters indicate that the complex assumes non-crystallographic molecular C_s symmetry within experimental error. The conformation of **3** deviates significantly from exact C_s symmetry: the pyrrolyl nitrogen deviates 6.7° from the central position.

The increased difficulty of rotation from Fe(Cp)$_2$ to [3,3′-Co(1,2-$C_2B_9H_{11}$)$_2$]$^-$ to [3-Co(η^5-NC_4H_4)-1,2-$C_2B_9H_{11}$]: Sandwich complex **1** is similar to ferrocene and [3,3′-Co(1,2-$C_2B_9H_{11}$)$_2$]$^-$. On the basis of its geometrical rotamer preferences in the solid state and solution, some questions on the rotational habits of the other two can be answered. The disposition of the hydrogen atoms on the π faces of the three sandwich complexes is emphasized in Figure 1. In Cp and in $[NC_4H_4]^-$, the C–H bonds are in the plane of the aromatic ring, whereas the B–H and C–H bonds are out of this plane and face the opposite ligand in the dicarbollide. It is then appropriate to assume that the steric energy will contribute more to the rotational barriers for the [3,3′-Co(1,2-$C_2B_9H_{11}$)$_2$]$^-$ ion than for the other two complexes. This does not mean, however, that the electronic contribution is too weak to discriminate between the different possible rotamers. Could this be estimated independently of the steric contribution? We think that the answer is obtained from the former experiments with **1**. The H···H repulsion energies between the two mutually rotating ligands are lower in **1** than in [3,3′-Co(1,2-$C_2B_9H_{11}$)$_2$]$^-$, and can be estimated comparably to those in ferrocene on the basis that H···H distances are close to 3 Å in eclipsed ferrocene and close to 2.7 Å in derivatives of **1**, both being longer than the sum of the van der Waals radii (2.4 Å), whereas H···H distances in eclipsed [3,3′-Co(1,2-$C_2B_9H_{11}$)$_2$]$^-$ would be near 2.1 Å. Therefore it may be assumed that the *cis* rotamer in **1** is influenced mainly by electronic factors. Considering that $[NC_4H_4]^-$ and $[7,8\text{-}C_2B_9H_{11}]^{2-}$ are very similar as η^5 ligands, and that the electronegativity difference between the constituent atoms within each ligand (0.5) is the same,[17] it can then be inferred that $[NC_4H_4]^-$ is like $[7,8\text{-}C_2B_9H_{11}]^{2-}$ with no steric implications. Accordingly, it seems reasonable that when electronic factors alone are considered [3,3′-Co(1,2-$C_2B_9H_{11}$)$_2$]$^-$ adopts a *cisoid* conformation, as does **1**. Why is the *cis* conformation so well defined in **1** and its derivatives, while it is much less so in [3,3′-Co(1,2-$C_2B_9H_{11}$)$_2$]$^-$ and in its derivatives? Avoiding the steric energies implicated, one possible answer lies in the neutral nature of **1** and the anionic nature of [3,3′-Co(1,2-$C_2B_9H_{11}$)$_2$]$^-$. The semiempirical calculations on **1** and its derivatives in the gas phase and the energy profiles reported here correlate very well with the experimental data. However in the [3,3′-Co(1,2-$C_2B_9H_{11}$)$_2$]$^-$ ion the interaction of the counterion with the electron-rich B–H moieties introduces additional types of forces to which the neat rotamer must adapt. This explains the dispersity of rotamers

found even in the plain [3,3′-Co(1,2-$C_2B_9H_{11}$)$_2$]$^-$ ion. If groups other than H occupy sites in the confronting faces of the [3,3′-Co(1,2-$C_2B_9H_{11}$)$_2$]$^-$ ion, the resulting rotamer is the combination of the different participating forces, including the steric repulsions.

The difference in rotational behavior between ferrocene and **1** can be explained by the pinning effect caused by the heteroatoms in **1**. It would be intriguing to know, however, why the N and C atoms in **1**, or all C atoms in [3,3′-Co(1,2-$C_2B_9H_{11}$)$_2$]$^-$, prefer to be in a *cis* or *cisoid* disposition, since our ZINDO calculations on the unreported [Fe(NC_4H_4)$_2$] have shown that the most stable conformation has both N atoms occupying a *trans* disposition. This rotamer is supported by the crystal structure of the related [Fe($C_4Me_4NBH_3$)$_2$] complex,[18] in which both N atoms occupy *trans* positions. The *trans* disposition of the heteroatoms in [Fe(NC_4H_4)$_2$] can be easily explained as it attenuates the coulombic repulsions that would originate from the negative N if they were in a *cis* configuration. In **1** and [3,3′-Co(1,2-$C_2B_9H_{11}$)$_2$]$^-$ there may be a *trans* influence, in which the more electronegative atoms prefer the more electropositive ones to be *trans* to them. This concept is supported by the fact that, once the metal ion is reduced, for example from d^6 to d^7, the *cisoid* arrangement is disfavored with regard to the *transoid*.[10c] On reduction of the complex, the extra charge accumulates on B8–H, producing a situation similar to that in [Fe(NC_4H_4)$_2$] (see Figure 11). The charge separation also

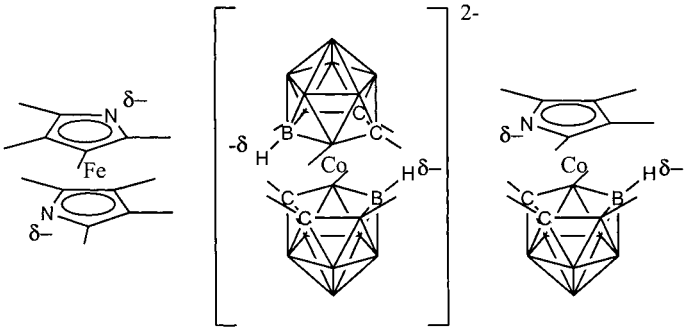

Figure 11. Rotamer stabilization by attenuation of the coulombic repulsions: in [Fe(NC_4H_4)$_2$], in d^7 [3,3′-Co(1,2-$C_2B_9H_{11}$)$_2$]$^{2-}$ and in [3-Co(η^5-NC_4H_4)-1,2-$C_2B_9H_{11}$] (**1**). B8 atoms are indicated in the dicarbollide ligands as B.

supports the *cis* conformation found for **1**. The rotamer adopted is the one with the atoms holding the negative charges furthest apart in all three complexes [Fe(NC_4H_4)$_2$], in d^7 [3,3′-Co(1,2-$C_2B_9H_{11}$)$_2$]$^{2-}$ and [3-Co(η^5-NC_4H_4)-1,2-$C_2B_9H_{11}$] (**1**).

Conclusion

By combination of ^{1}H DNMR experiments, the synthesis of *closo*-[3-Co(η^5-NC_4H_4)-1,2-$(CH_3)_2$-1,2-$C_2B_9H_9$] (**2**) and *closo*-[3-Co(η^5-NC_4H_4)-1,2-(μ-CH_2)$_3$-1,2-$C_2B_9H_9$] (**3**), the formation of adducts **2**→BF_3 and **3**→BF_3, and computational studies of the relative energy of the different rotamers it has been possible to demonstrate unambiguously that, contrarily to ferrocene, *closo*-[3-Co(η^5-NC_4H_4)-1,2-$C_2B_9H_9$] (**1**) exists as only one rotamer at room and lower temperatures. This rotamer, $\mathbf{A_2}$, has the nitrogen atom bisecting the dicarbollide $C_c\cdots C_c$ edge; therefore it has a *cis* configuration and it matches very well with the molecular structures determined by X-ray analysis of **1**, **2**, and **3**. Other rotamers of **1** are very high in energy and inaccessible by common laboratory reaction setups. Therefore, **1** represents the first sterically unencumbered sandwich complex with a well-defined conformation,[19] practically 100% populated at room temperature. Its rigidity, its Co^{III}/Co^{II} electrochemical behavior, its N–σ coordination capacity, its practical synthesis, and the possibility of substitution at the α-pyrrolyl carbon atoms and/or at the dicarbollide cluster atoms makes this compound attractive for molecular engineering or molecular motor design.[10c]

The stability of rotamer $\mathbf{A_2}$ was proven by substitutions on the pyrrolyl and/or the dicarbollide unit. No modification of the stability of $\mathbf{A_2}$ relative to more energetic rotamers was obtained, either when the BF_3 group was bonded to the pyrrolyl nitrogen or when substituents were placed on the cluster carbon atoms. Only when three substituents were placed on the same triangular face, on the pyrrolyl nitrogen and on the two carbon cluster atoms, were new racemic rotamers ($\mathbf{A_g}$ and $\mathbf{A_r}$) co-existing with rotamer $\mathbf{A_1}$ found both experimentally and by computational methods. It can be concluded that **1** and its derivatives are found at room temperature in only one rotamer, $\mathbf{A_2}$, and by adequate substitution two other conformers, $\mathbf{A_1}$ and $\mathbf{A_g}$/$\mathbf{A_r}$, can be forced to co-exist with it.

The *cis* disposition of its heteroatoms prompts comparison of **1** with two other related sandwich complexes: ferrocene and [3,3′-Co(1,2-$C_2B_9H_{11}$)$_2$]$^-$. The presence of one heteroatom in **1** pins the pyrrolyl ligand into a fixed conformation; this is impossible in ferrocene, which consequently has a lower rotational barrier. The fixed conformation of **1** also assists in defining the rotational preferences of [3,3′-Co(1,2-$C_2B_9H_{11}$)$_2$]$^-$ in the absence of steric hindrance. The latter is *cisoid*, and the diversity of structures found, with many different orientations of the cluster C atoms, should be attributed to its anionic nature, which requires a cation. Attractive forces between this cation and B–H groups in the cluster determine the different rotamers found in the solid phase.

This research also draws attention to the singularity of the three electronegative atoms in **1** occupying the same region of space, thence producing a *cis* rotamer. This has been interpreted as a *trans* influence originating in the electropositive character of the boron.

Experimental Section

Instrumentation: Elemental analyses were performed with a Carlo Erba EA 1108 microanalyzer. IR spectra were recorded with KBr pellets on an

FTIR-8300 Shimadzu spectrophotometer. ^{1}H, ^{1}H{^{11}B}, ^{13}C{^{1}H}, ^{11}B, and ^{11}B{^{1}H} NMR spectra were recorded at room temperature with a Bruker ARX300 instrument equipped with the appropriate decoupling accessories. Low-temperature measurements were performed in $(CD_3)_2CO$. Sample temperatures were maintained with a B-VT2000 digital temperature controller by means of a thermocouple situated in the cooling gas a few centimeters below the sample, and accurate to within ± 0.5 °C over the dynamic temperature range.

Materials: Experiments were carried out under a dry, oxygen-free dinitrogen atmosphere, using standard Schlenk techniques, with some subsequent manipulation in the open atmosphere. THF was freshly distilled from sodium benzophenone. Other solvents were of reagent grade and were used without further purification. Pyrrole (Aldrich) was freshly distilled before use. Hexahydrated cobalt(II) chloride (Aldrich) was heated under vacuum overnight to obtain the anhydrous form. Potassium was refluxed in THF before use. $(C_2H_5)_2O\rightarrow BF_3$ (Fluka) and 1-CH_3-1,2-$C_2B_{10}H_{11}$ and 1,2-$C_2B_{10}H_{12}$ (Katchem) were used as received. 1,2-$(CH_3)_2$-1,2-$C_2B_{10}H_{10}$,[20] 1,2-$(\mu$-$CH_2)_3$-1,2-$C_2B_{10}H_{10}$,[21] and *closo*-[3-Co(η^5-NC_4H_4)-1,2-$C_2B_9H_{11}$][12] (**1**) were prepared according to literature methods.

Synthesis of *closo*-[3-Co(η^5-NC_4H_4)-1,2-$(CH_3)_2$–1,2-$C_2B_9H_9$] (2): 1,2-$(CH_3)_2$-1,2-$C_2B_{10}H_{10}$ (0.15 g, 0.87 mmol) was dissolved in a suspension of K[NC_4H_4] (1.10 g, 10.4 mmol) in THF (50 mL). After 4 h of refluxing, anhydrous $CoCl_2$ (0.57 g, 4.3 mmol) was added. The reaction mixture was refluxed for 48 h. After cooling, the solvent was removed inder vacuum, and the resulting solid was extracted with dichloromethane (50 mL). The suspension was filtered and the resulting dark liquid was evaporated to 1 mL and chromatographed over silica gel using dichloromethane/hexane (8:2) as mobile phase. A pure orange complex was obtained (R_f(prep) = 0.70). Yield: 0.14 g, 56%. Elemental analysis calcd (%) for $C_8B_9H_{19}CoN$ (226.6): C 33.66, H 6.71, N 4.91; found: C 33.81, H 6.90, N 4.73; IR (KBr): $\tilde{\nu}$ = 2592, 2559, 2542 cm^{-1} (B–H); ^{1}H NMR (300 MHz, $(CD_3)_2CO$, 25 °C, TMS): δ = 7.0 (s, 2H; N–C_{pyr}–H), 6.5 (s, 2H; C_{pyr}–C_{pyr}–H), 2.5 ppm (s, 6H; CH_3); ^{1}H{^{11}B} NMR (300 MHz, $(CD_3)_2CO$, 25 °C, TMS): δ = 7.0 (s, 2H; N–C_{pyr}–H), 6.5 (s, 2H; C_{pyr}–C_{pyr}–H), 3.7 (brs, 2H; B–H), 3.2 (brs, 2H; B–H), 2.5 (s, 6H; CH_3), 2.1 (brs, 1H; B–H), 1.5 (brs, 2H; B–H), 1.0 ppm (brs, 2H; B–H); ^{13}C{^{1}H} NMR (75.5 MHz, $(CD_3)_2CO$, 25 °C, TMS): δ = 115.4 (s; N–C_{pyr}), 91.0 (s; C_{pyr}–C_{pyr}), 79.4 (s; C_c), 29.5 ppm (s; CH_3); ^{11}B NMR (96.3 MHz, $(CD_3)_2CO$, 25 °C, $(C_2H_5)_2O\rightarrow BF_3$): δ = 5.5 (d, ^1J(B,H) = 139 Hz, 1B), 4.1 (d, ^1J(B,H) = 140 Hz, 1B), −0.4 (d, ^1J(B,H) = 155 Hz, 2B), −5.8 (d, ^1J(B,H) = 144 Hz, 2B), −11.6 ppm (d, ^1J(B,H) = 160 Hz, 3B).

Synthesis of *closo*-[3-Co(η^5-NC_4H_4)-1,2-(μ-$CH_2)_3$-1,2-$C_2B_9H_9$] (3): The procedure was the same as for **2** but with 1,2-(μ-$CH_2)_3$-1,2-$C_2B_{10}H_{10}$ (0.16 g, 0.87 mmol) as starting material. R_f(prep) = 0.70. Yield: 0.14 g, 54%. Elemental analysis: calcd (%) for $C_9B_9H_{19}CoN$ (238.6): C 36.34, H 6.44, N 4.71; found: C 36.60, H 6.30, N 4.81; IR (KBr): $\tilde{\nu}$ = 2596, 2557, 2546 cm^{-1} (B–H); ^{1}H NMR (300 MHz, $CDCl_3$, 25 °C, TMS): δ = 6.6 (s, 2H; N–C_{pyr}–H), 6.3 (s, 2H; C_{pyr}–C_{pyr}–H), 2.6 (m, 4H; C_c–CH_2–), 2.5 ppm (m, 2H; CH_2); ^{1}H{^{11}B} NMR (300 MHz, $CDCl_3$, 25 °C, TMS): δ = 6.6 (s, 2H; N–C_{pyr}–H), 6.3 (s, 2H; C_{pyr}–C_{pyr}–H), 3.6 (brs, 2H; B–H), 3.2 (brs, 1H; B–H), 2.6 (m, 4H; C_c–CH_2–), 2.5 (m, 2H; CH_2), 1.9 (brs, 2H; B–H), 1.6 (brs, 2H; B–H), 1.2 ppm (brs, 2H; B–H); ^{13}C{^{1}H} NMR (75.5 MHz, $CDCl_3$, 25 °C, TMS): δ = 109.1 (s; N–C_{pyr}), 83.8 (s; C_{pyr} – C_{pyr}), 34.2 (s; C_c–CH_2), 26.1 ppm (s; –CH_2–); ^{11}B NMR (96.3 MHz, $CDCl_3$, 25 °C, $(C_2H_5)_2O\rightarrow BF_3$): δ = 8.2 (d, ^1J(B,H) = 157 Hz, 1B), 7.0 (d, ^1J(B,H) = 134 Hz, 1B), −3.2 (d, ^1J(B,H) = 157 Hz, 2B), −6.5 (d, ^1J(B,H) = 148 Hz, 2B), −11.6 ppm (d, ^1J(B,H) = 161 Hz, 3B).

Adduct formation monitored by proton and boron NMR spectra: The three complex–BF_3 adducts **1**→BF_3, **2**→BF_3, and **3**→BF_3 were prepared by adding $(C_2H_5)_2O\rightarrow BF_3$ (0.1 mmol) to three solutions of 0.1 mmol of complexes **1–3** (28.5, 29.7, and 25.7 mg respectively) in $(CD_3)_2CO$ (1 mL). The cobaltacarborane complexes **1–3** were weighed on a microbalance and a measured volume of $(CD_3)_2CO$ was added. The resulting bright orange solutions were stirred for 1 min and carefully transferred to a 5 mm NMR tube, where the ^{1}H DNMR measurements were performed. Experimental evidence for the formation of the adducts has been presented earlier.[22]

Computational details: All calculations were performed using the Hyperchem 5.0 package (Version 5.0, Hypercube Inc.) installed on a PC Pentium III 700 MHz computer. Internal coordinates obtained from X-ray diffraction analysis of complexes **1**,[12] **2**, and **3** were used as starting coordinates. Three geometrical operations were performed before the calculations were started: 1) the pyrrolyl plane and the pentagonal open face of the cluster were forced to be parallel; 2) the nitrogen atom was placed exactly halfway between the C_c atoms; 3) the BF_3 boron–nitrogen distance in **1**→BF_3, **2**→BF_3, and **3**→BF_3 was fixed at 1.598 Å.[18]

From the starting position, rotations of 9° were performed (from α = 9° to α = 180°). At each point, a single-point calculation was performed using the ZINDO/1 semiempirical method. Before the ZINDO calculations, the cluster carbons, the fluorine atoms, and the *exo* cluster substituents were allowed to relax by means of molecular mechanics geometry optimization. All energy values correspond to free enthalpy referred to the lowest-energy rotamer.

X-ray diffraction studies

Structure determinations of 2 and 3: Single-crystal data collections were performed at room temperature on a Rigaku AFC5S diffractometer using graphite-monochromated $Mo_{K\alpha}$ radiation. A total of 2556 and 1499 unique reflections were collected by $\omega/2\theta$ scan mode ($2\theta_{max}$ = 50°) for **2** and **3**, respectively. Crystallographic data are presented in Table 3.

The structures were solved by direct methods and refined on F^2 by the SHELX-97 program.[23] Non-hydrogen atoms, except boron atoms of **3**, were refined with anisotropic displacement parameters and hydrogen atoms were placed at calculated positions and treated as riding atoms.

CCDC-177729 and CCDC-177730 contain the supplementary crystallographic data for this paper. These data can be obtained free of charge from The Cambridge Crystallographic Data Centre via www.ccdc.cam.ac.uk/data_request/cif.

Acknowledgements

This work was supported by CICYT (Projects MAT01–1575 and MAT1999–1815-CE), Generalitat de Catalunya (Grants 1998FI 00724 and 2001/SGR/00337).

[1] Representative examples: a) T. J. Kealy, P. L. Pauson, *Nature* **1951**, *168*, 1039–1040; b) S. A. Miller, J. A. Tebboth, J. F. Tremaine, *J. Chem. Soc.* **1952**, 632–635.

[2] Representative examples: a) T. Hayashi in *Ferrocenes* (Eds.: A. Togni, T. Hayashi), VCH, Weinheim, **1995**, p. 118, and references therein; b) *J. Organomet. Chem.* **2001**, *637–639*, 1–875 (special issue to mark the 50th Anniversary of the first report of the compound ferrocene).

[3] Representative example: N. Kuhn, K. Jendral, S. Stubenrauch, R. Mynott, *Inorg. Chim. Acta* **1993**, *206*, 1–3.

[4] Representative example: a) L. N. Mulay, A. Attalla, *J. Am. Chem. Soc.* **1963**, *85*, 702–706; b) S. Sorriso, G. Cardaci, S. M. Murgia, *J. Organomet. Chem.* **1972**, *44*, 181–184.

[5] Representative example: L. Goodman, H. Gu, V. Pophristic, *J. Chem. Phys.* **1999**, *110*, 4268–4275.

[6] a) M. Hillman, J. D. Austin, *Organometallics* **1987**, *6*, 1737–1743; b) I. R. Butler, W. R. Cullen, *Can. J. Chem.* **1989**, *67*, 1851; c) K. Onitsuka, T. Yoshida, A. Ichimura, T. Adachi, T. Yoshida, K. Sonogashir, *Chem. Lett.* **1995**, *6*, 427; d) S. L. Ingham, N. J. Long, *Angew. Chem.* **1994**, *106*, 1847–1848; *Angew. Chem. Int. Ed. Engl.* **1994**, *33*, 1752–1753; e) E. Herdtweck, F. Jäkle, M. Wagner, *Organometallics* **1997**, *16*, 4737–4745; f) R. W. Heo, T. R. Lee, *J. Organomet. Chem.* **1999**, *578*, 31–42.

[7] a) *Contemporary Boron Chemistry* (Eds.: M. Davidson, A. K. Hughes, T. B. Marder, K. Wade), Royal Society of Chemistry, Cambridge, **2000**; b) *Advances in Boron Chemistry* (Ed.: W. E. Siebert), Royal Society of Chemistry, Cambridge, **1997**; c) *The Borane–Carborane–Carbocation Continuum* (Ed.: J. Casanova), Wiley-Inter-

science, New York, **1998**; d) *Comprehensive Organometallic Chemistry II*, *Vol. 1* (Eds.: E. W. Abel, F. G. A. Stone, G. Wilkinson), Pergamon Press, Oxford, UK, **1995**; e) *Boron Chemistry at the Beginning of the 21st Century* (Ed.: Yu. N. Bubnov), Editorial URSS, Moscow, **2003**.

[8] a) K. K. Joshi, P. L. Pauson, A. R. Qazi, W. H. Stubbs, *J. Organomet. Chem.* **1964**, *1*, 471–475; b) L. N. Ji, D. L. Kershner, M. E. Rerek, F. Basolo, *J. Organomet. Chem.* **1985**, *296*, 83–94; c) D. N. Kursanov, V. N. Setkina, N. I. Pyshnograeva, *Bull. Acad. Sci. USSR Div. Chem. Sci. (Engl. Transl.)* **1984**, *33*, 807, and references therein; d) J. Zakrzewski, C. Giannotti, *Coord. Chem. Rev.* **1995**, *140*, 169–187, and references therein.

[9] a) N. Kuhn, E. M. Horn, E. Zauder, D. Blaser, R. Boese, *Angew. Chem.* **1988**, *100*, 572–573; *Angew. Chem. Int. Ed. Engl.* **1988**, *27*, 579–580; b) K. J. Chase, R. F. Bryan, M. K. Woode, R. N. Grimes, *Organometallics* **1991**, *10*, 2631–2642; c) R. J. Butcher, W. L. Darby, E. Sinn, *Inorg. Chim. Acta* **1993**, *203*, 51–54; d) I. B. Sivaev, V. I. Bregadze, *Collect. Czech. Chem. Commun.* **1999**, *95*, 783–805, and references therein.

[10] a) A. Zalkin, T. E. Hopkins, D. H. Templeton, *Inorg. Chem.* **1967**, *6*, 1911–1915; b) R. M. Chamberlin, B. L. Scott, M. M. Melo, K. D. Abney, *Inorg. Chem.* **1997**, *36*, 809–817; c) M. F. Hawthorne, J. I. Zink, J. M. Skelton, M. J. Bayer, C. Liu, E. Livshits, R. Baer, D. Neuhauser, *Science* **2004**, *303*, 1849–1851.

[11] L. Borodinsky, E. Sinn, R. N. Grimes, *Inorg. Chem.* **1982**, *21*, 1686–1689.

[12] M. Lamrani, S. Gómez, C. Viñas, F. Teixidor, R. Sillanpää, R. Kivekäs, *New J. Chem.* **1996**, *20*, 909–912.

[13] a) F. Teixidor, S. Gómez, M. Lamrani, C. Viñas, R. Sillanpää, R. Kivekäs, *Organometallics* **1997**, *16*, 1278–1283; b) S. Gómez, C. Viñas, M. Lamrani, R. Kivekäs, R. Sillanpää, *Inorg. Chem.* **1997**, *36*, 3565–3567; c) R. Sillanpää, J. Llop, C. Viñas, F. Teixidor, R. Kivekäs, *Acta Crystallogr. C* **2001**, *57*, 900–901; d) J. Llop, C. Viñas, F. Teixidor, L. Victori, R. Kivekäs, R. Sillanpää, *Organometallics* **2001**, *20*, 4024–4030; e) J. Llop, C. Viñas, F. Teixidor, L. Victori, R. Kivekäs, R. Sillanpää, *Organometallics* **2002**, *21*, 355–361; f) J. Llop, C. Viñas, F. Teixidor, L. Victori, R. Kivekäs, R. Sillanpää, *Inorg. Chem.* **2002**, *41*, 3347–3352.

[14] P. W. Atkins in *Concepts in Physical Chemistry*, Oxford University Press, Oxford, **1995**.

[15] $\mathbf{A_g}$ and $\mathbf{A_r}$ are enantiomers. Their rapid interchange produces a symmetrical unique species of average C_s symmetry.

[16] H. Friebolin in *Basic One- and Two-Dimensional NMR Spectroscopy*, VCH, New York, **1993**.

[17] In $[NC_4H_4]^-$ the electronegativity difference between N and C is 0.5; the electronegativity difference between C and B is also 0.5 in$[7,8\text{-}C_2B_9H_{11}]^{2-}$.

[18] N. Kuhn, E. M. Horn, R. Boese, N. Augart, *Angew. Chem.* **1989**, *101*, 354–355; *Angew. Chem. Int. Ed. Engl.* **1989**, *28*, 342–344.

[19] Earlier studies with dicarbollide half-sandwich complexes had already shown certain preferred dispositions of the ancillary ligands. a) T. B. Marder, R. T. Baker, J. A. Long, J. A. James, M. F. Hawthorne, *J. Am. Chem. Soc.* **1981**, *103*, 2988–2994; b) T. B. Marder, R. T. Baker, J. A. Long, J. A. James, M. F. Hawthorne, *J. Am. Chem. Soc.* **1982**, *104*, 4506; c) A. S. Batsanov, A. V. Churakov, J. A. K. Howard, A. K. Hughes, A. L. Johnson, A. J. Kingsley, I. S. Neretin, K. Wade, *J. Chem. Soc. Dalton Trans.* **1999**, *21*, 3867–3875.

[20] T. L. Heying, J. W. Ager, S. L. Clark, D. J. Mangold, H. L. Goldstein, M. Hillman, R. J. Polak, J. W. Szymanski, *Inorg. Chem.* **1963**, *2*, 1089–1092.

[21] T. E. Paxson, M. K. Kaloustian, G. M. Tom, R. J. Wiersema, M. F. Hawthorne, *J. Am. Chem. Soc.* **1972**, *94*, 4882–4888.

[22] J. Llop, F. Teixidor, C. Viñas, L. Victori, *J. Chem. Soc. Dalton Trans.* **2002**, *8*, 1559–1565.

[23] G. M. Sheldrick, SHELX-97, University of Göttingen, Germany, **1997**.

Received: May 6, 2004
Revised: November 12, 2004
Published online: February 1, 2005

